

Validation of an UV inversion algorithm using satellite and surface measurements

Pucaí Wang, Zhanqing Li, and Josef Cihlar

Canada Centre for Remote Sensing, Ottawa

David I. Wardle and J. Kerr

Atmospheric Environment Service, Downsview, Ontario, Canada

Abstract. Ultraviolet radiation in the spectral region between 280 and 315 nm (often referred to as UV-B) is harmful to living organisms. Satellite-based estimation of surface UV-B supplements the sparsely distributed ground-based UV-B monitoring networks. This study is concerned with validation of an inversion algorithm [Li *et al.*, this issue] for retrieving spectrally integrated UV-B (no spectral weighting) and erythemal UV (EUV) (with spectral weighting) fluxes at the surface from satellite. The physical inversion algorithm contains a few analytical expressions and input parameters: the solar zenith angle, ozone amount, albedo at the top of the atmosphere (TOA), and aerosol variables. The algorithm is applied to satellite measurements of total ozone amount and 360 nm reflectance from Meteor 3/TOMS and visible reflectance from NOAA/AVHRR. The retrieved UV-B and EUV fluxes are compared with ground UV observations made at six Canadian UV observation stations with Brewer instruments from 1992 to 1994. Under all-sky conditions the comparisons showed very small mean differences and relatively large standard deviations (s.d.): 0.033 W/m² (mean) and 0.287 W/m² (s.d.) for total UV-B and 3.02 mW/m² (mean) and 12.0 mW/m² (s.d.) for EUV radiation. The large standard deviations are attributed to the inhomogeneity in sky condition and mobility of cloudy scenes, which renders an inaccurate match between satellite and surface measurements. The comparisons under clear-sky conditions showed very small mean and standard differences. By means of a running average over a period of time, satellite inversion can track the variation of surface-observed UV-B and EUV very well.

1. Introduction

The discovery of the ozone hole in the Antarctica [Farman *et al.*, 1985; Solomon, 1988] and the continuous ozone decrease in high and middle latitudes [WMO, 1994; Bojkov *et al.*, 1990; McPeters *et al.*, 1996; Wardle *et al.*, 1997] have spawned much concern about the potential increase of harmful UV-B radiation. High UV dose rates can have a serious biological effect on human skin and DNA and ocean and forest ecosystems [Madronich, 1993; Setlow, 1974; Caldwell, *et al.*, 1986; McKinlay *et al.*, 1987]. Many efforts have been made to observe the trend of surface UV-B radiation using both spectral and broadband measurements [Webb *et al.*, 1997; Bigelow *et al.*, 1988; Wardle *et al.*, 1996; Booth *et al.*, 1995; McKenzie *et al.*, 1995]. A remarkable increase in UV-B has been reported in the polar region where a significant loss of stratospheric ozone occurred [Herman *et al.*, 1996]. An increasing trend in UV-B has also been detected in some middle-latitude areas. However, identification of the causes for the trend in middle-latitude regions is complicated by the changes in cloud and aerosol, as well as by some increase in tropospheric ozone [Kerr *et al.*, 1993; Lubin *et al.*, 1995].

Ground-based instruments provide in situ measurements of current and historical UV-B over restricted regions. There are many practical impediments to the deployment of extensive

ground-based observation networks. Currently, there are two popular types of ground instruments measuring UV. Easily maintained broadband instruments such as Robertson-Berger meters provide observations of some spectrally integrated UV dose rates. They do not, however, allow one to compute any biological UV dose rates. This shortcoming is overcome by UV spectroradiometers such as the widely used Brewer instruments that measure UV irradiance at various wavelengths. The UV dose rate can be derived by convolving the spectral observations with a biological action spectrum. In addition to the provision of UV dose rates, spectrometer data are used to gain information on ozone and aerosol, two major variables altering surface UV intensity [Mayer *et al.*, 1997; Mayer and Seckmeyer, 1996]. Despite many limitations, surface UV measurement provides a benchmark database for validating satellite estimation.

A practical method for efficient derivation of global surface UV-B from Nimbus Total Ozone Mapping Spectrometer (TOMS) was proposed by Eck *et al.* [1995]. Their method first computes surface UV-B irradiance for clear atmosphere based on a radiative transfer model [Dave, 1964]. UV-B irradiances for cloudy sky conditions were calculated by introducing a cloud correction factor derived from TOMS reflectivity data at 360 nm or 380 nm. Aerosol attenuation effects were included by Krotkov *et al.* [1998] with an aerosol correction factor, similar to that for clouds, for cloud-free sky conditions. The algorithm can retrieve both spectrally resolved and integrated UV-B irradiances.

Copyright 2000 by the American Geophysical Union.

Paper number 1999JD900403.
0148-0227/00/1999JD900403\$09.00

An alternative inversion algorithm that explicitly accounts for the effects of all major factors influencing the transfer of UV radiation was recently proposed by *Li et al.*, [this issue]. It was developed on the basis of a simplified radiative transfer model and validated against a full fledged DISORT-based UV radiative transfer model [*Wang and Lenoble*, 1994, 1996; *Wang*, 1995]. Using “satellite observations” as simulated by a full-fledged radiative transfer model as input data, the simple inversion algorithm can derive surface UV-B fluxes that are in excellent agreement with those simulated by the detailed model under a wide range of conditions with those obtained by the model [*Li et al.*, this issue]. The algorithm is tested in this study with real observation data collected across Canada from 1992 to 1994. The algorithm is of great potential for operational application over large areas and for a long period of observation, due to its simplicity and very few input parameters required. The major input variables are total ozone amount, albedos at the top of the atmosphere (TOA) and at the surface, and aerosol optical properties. Accuracy and efficiency are two major concerns for operational retrieval of UV fluxes. Spaceborne observation of ozone and UV has a rather long history [*McPeters et al.*, 1993]. For example, TOMS data have been available since 1978 onboard Nimbus 7 till 1993, and on Meteor 3 during 1991–1994, on the Japanese ADEOS during 1996–1997, and on the current Earth probe. With ozone information, surface UV fluxes can actually be retrieved from any satellite measurements at nonozone absorption bands such as the visible channel of the advanced very high resolution radiometer (AVHRR).

The following section describes in more detail both satellite and surface data sets employed in this study, followed by an outline of the inversion algorithm. Section 4 presents the results of comparisons and discussions concerning the discrepancies. The study is concluded in section 5.

2. Data

2.1. Ground Observation

The UV ground measurements collected in Canada have been employed in several satellite validation studies [*Eck et al.*, 1987; *Krotkov et al.*, 1998]. The Canadian UV stations are listed in Table 1. They were all equipped with the same instrument, namely, the Brewer spectrophotometer [*Kerr et al.*, 1995]. Most stations are located in open areas, surrounded by trees, meadows, or low houses. However, Toronto station is slightly blocked in one direction with an inclination angle of 8° above the horizon. Its effect is negligible on surface UV irradiance measurements except for near sunrise or sunset, which are not used in this investigation. The data quality was controlled following some strict operation procedures. Absolute calibration was performed about 6 times per year with 1000-W standard

lamps for the Toronto Brewer instrument 14 and once every one or two years for other instruments by the same standard lamps and one traveling Brewer instrument to the site. The lamps are traceable to the U.S. National Institute of Standards and Technology (NIST). Radiometric stability was checked daily with an internal 20-W quartz halogen lamp. Wavelength check was carried out several times a day with reference to a mercury discharge lamp. Stray light was carefully removed. However, wavelength-dependent effect up to 4% over the operating range of temperature remained. For the Toronto Brewer the spectral responsivity drifts about 0.3–1.0% per year in comparison with 1000-W standard lamp readings [*Wardle and Kerr*, 1996]. The maximum uncertainty for wavelength was 0.05 nm and for radiance was 6% for the central station (Toronto) and 7% for field stations. All data, flagged as being bad quality by the producers, were excluded from the validation. Surface downwelling UV-B irradiances were obtained by integrating spectral UV irradiance measurements over the UV-B range (280–320 nm), while EUV fluxes result from integration weighted by the erythemal action spectrum over the range 280–400 nm.

2.2. Satellite Observation

While the inversion algorithm was adapted for readily use with TOMS data, it is applicable to any satellite sensor whose measurements are highly correlated with TOA UV albedo data, provided total ozone amounts are known. To demonstrate this, two types of satellite data, TOMS and AVHRR, are employed. The estimated UV-B and EUV are compared with ground observations. Total ozone amounts derived from TOMS were used to calculate UV-B ozone transmission. Reflectance measurements from TOMS 360 nm channel and AVHRR visible channel were converted to TOA UV albedos following spectral and angular corrections. The TOA albedos denote the effects of atmospheric scattering due to air molecules, cloud, and aerosol particles.

The Meteor-3 TOMS data obtained between 1992 and 1994 were matched with ground measurements at the Canadian UV stations. Unlike Sun-synchronous satellites having fixed local overpass time, Meteor 3 provides measurements at various local times of different solar angles so that its effect on the retrieval may be evaluated. The bulk of surface Brewer data was collected after 1990 at most stations. TOMS measured backscattered radiance by the Earth’s surface and atmosphere at three ozone-sensitive and three insensitive wavelengths: 312.35, 317.40, 331.13, 339.73, 360, and 380.16 nm [*McPeters et al.*, 1993; *Herman et al.*, 1996]. Total ozone amount was retrieved from TOMS. The TOMS has an instantaneous field of view (IFOV) on the Earth’s surface of about 50 × 50 km² at nadir. The TOMS level-2 data set in hierarchical data format (HDF) was used. This includes observed backscattered radiances at the six wavelengths, retrieved total ozone amount, solar zenith angle (SZA), view zenith angle (VZA), relative azimuth angle (RAA), cloud fraction, and data-quality flags.

The National Oceanographic and Atmospheric Administration (NOAA) AVHRR data acquired in 1994 were also employed for estimating surface UV radiation. The AVHRR radiometer scans the Earth in a cross-tracking mode with a maximum scan angle of 55.4°. The field of view degrades from a circle with a 1.1 km diameter at nadir to an ellipse (2.5 km × 6.8 km in size) at the largest scanning angle. AVHRR has five channels, but only the visible reflected radiances (0.58–0.68 μm) were employed here. The AVHRR data are received at

Table 1. Canadian UV Monitoring Stations

Code	Name	Latitude, °N	Longitude, °W	Elevation, m
14	Toronto	43.78	79.47	198
84	Halifax	44.74	63.67	31
83	Winnipeg	49.90	97.24	239
71	Regina	50.21	104.71	592
13	Edmonton	53.55	114.10	766
19	Saturna	48.78	123.13	178

the Prince Albert satellite-receiving station in Saskatchewan, Canada, and cover most of the Canadian landmass except for a small portion of the Atlantic Provinces. The data were calibrated using postlaunch time-dependent gain and offset coefficients [Cihlar and Teillet, 1995]. Data registration was done with reference to ground control points obtained from high-resolution image chips. In addition to radiance measurements, three illumination/observation angles, namely SZA, VZA, and RAA, were also available.

Note that these space-borne sensors observed radiances reflected in a particular direction, while the inversion algorithm of Li *et al.* [this issue] requires TOA albedo, a ratio of the reflected irradiance in the entire upper hemispheric domain over the incoming downward irradiance. Albedo and reflectance (also referred to as bidirectional reflectance) are usually not identical, albeit a Lambertian reflector. For a given scene type, albedo is a function of SZA only denoted by $A(\theta_0)$, while reflectance is a function of all three angles $a(\theta_0, \theta, \phi)$. Albedos can be estimated from reflectances using angular dependence model (ADM) $R(\theta_0, \theta, \phi)$ [Li, 1996]:

$$A(\theta_0) = \frac{a(\theta_0, \theta, \phi)}{R(\theta_0, \theta, \phi)}. \quad (1)$$

At present, there were few sets of TOA ADMs for variable sky and surface scene conditions. Most notably is that developed for the Earth Radiation Budget Experiment (ERBE) using data primarily from the Nimbus-7 Earth Radiation Budget data [Suttles *et al.*, 1988]. There are 12 ERBE ADMs corresponding to 12 scene types with four cloud classes over different surface types. The cloud categories are determined by cloud amount (clear, 0–5%; partly cloud, 5–50%; mostly cloudy, 50–95%; and overcast cloud, >95%) which is part of the TOMS level-2 product. While the ERBE ADMs were designed for broadband shortwave measurements, they are substituted here for UV-B as the first approximation. Further work is under way to assess the ensuing uncertainties.

3. Satellite-Retrieving Algorithm

The algorithm that Li *et al.* [this issue] developed for retrieving both surface UV-B irradiance and erythemal weighted UV flux is summarized below.

$$UV_{SFC}^{\downarrow} = UV_{SFC}^{\downarrow}(1 - A_s) \quad (2)$$

$$UV_{SF} = (1 - a - bR_{360} - A_2)CT_{O_3,eff}UV_{TOA}^{\downarrow} \quad (3)$$

$$C = \frac{(1 - A_s)}{(1 - A_s) + A_2^*A_s}, \quad (4)$$

$$A_2 = 1 - \exp(-a_2\tau_a), \quad (5)$$

$$A_2^* = 1 - \exp(-b_2\tau_a), \quad (6)$$

$$\tau_a = (1 - \omega_0)\tau_e, \quad (7)$$

where UV_{SFC}^{\downarrow} and UV_{SFC} denote downwelling and net UV fluxes at the surface for either UV-B or EUV, respectively. R_{360} is the TOA albedo at 360 nm, $T_{O_3,eff}$ is the band-mean transmittance due to ozone absorption, UV_{TOA}^{\downarrow} is UV irradiance incident at the TOA, A_s is surface albedo, ω_0 is aerosol single-scattering albedo, τ_e is aerosol optical thickness due to both scattering and absorption, τ_a is same as τ_e but for absorption only. The coefficients for total UV-B are $a = 0.196$, $b = 0.798$, $a_2 = 1.33$, $b_2 = 1.66$, while for erythemal UV,

they are equal to 0.193, 0.817, 1.15, and 1.66, respectively. These coefficients were derived under a wide range of atmospheric and surface conditions [Li *et al.*, this issue].

Each of the terms in the equations has a clear physical meaning and represents a basic UV radiative transfer process. For example, R_{360} denotes attenuation due to major scattering processes caused by atmospheric molecules, cloud and aerosol particles, and the Earth's surface. A_2 accounts for UV reduction due to aerosol absorption, $T_{O_3,eff}$ for ozone absorption, C for multiple reflection, and absorption between the aerosol and the surface layers. Therefore (3) indicates that surface UV fluxes are determined by solar UV irradiance incident at TOA, the band-mean ozone transmittance and a scattering factor related to air molecules, clouds and aerosols, and the surface. For nonabsorbing aerosols, A_2 becomes zero. For very low surface albedo the coefficient C is close to 1. In this case, the equation becomes even simpler. This is largely because the bulk of scattering and absorbing processes governing the UV transfer take place in separate layers. As a result, the majority of scattering media (bulk of air molecules, cloud particles, aerosol scatters, and Earth surface) can be treated as a single layer although their physical locations may be far apart, e.g., cloud and the surface. Their integrated effect is represented by

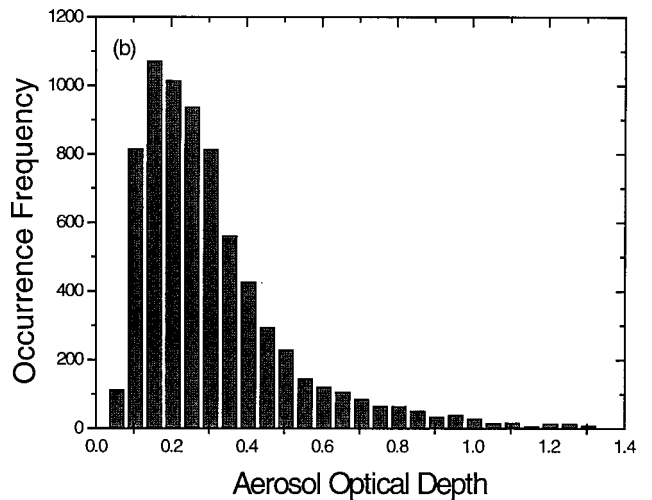
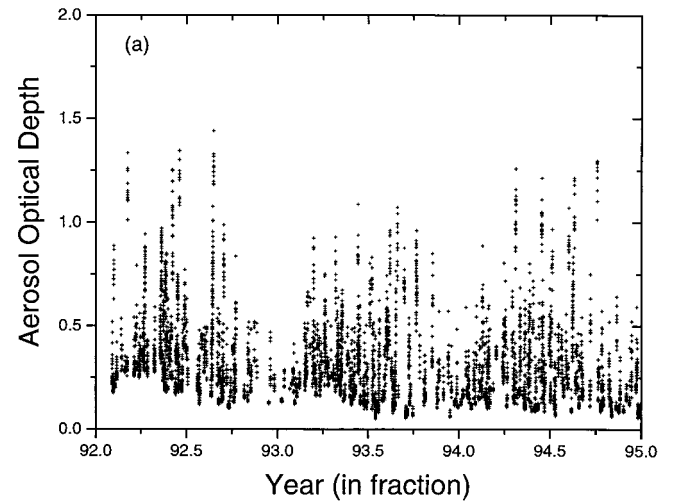


Figure 1. (a) Annual variation and (b) frequency distribution of aerosol optical depth in UV-B band in Toronto from 1992 to 1994.

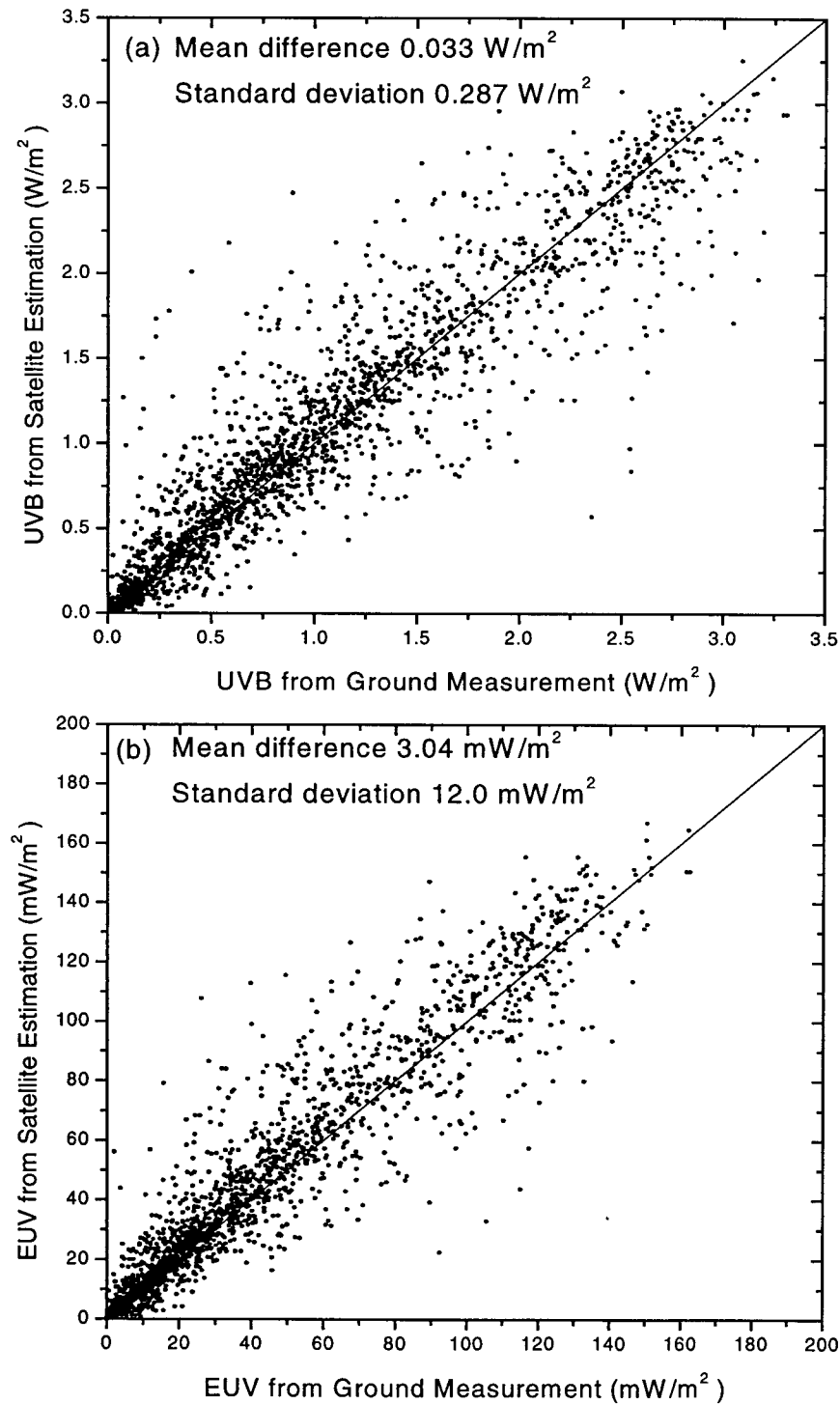


Figure 2. Comparisons between satellite-retrieved and ground-measured surface total (a) UV-B and erythemal (b) UV under all-sky conditions from 1992 to 1994. Satellite estimation was made using TOMS data, while surface data are from Canadian UV stations.

the reflectivity at any nonozone absorption band, such as the TOMS 360 nm band. AVHRR visible albedo R_{VIS} is highly correlated with R_{360} according to model simulations [Li *et al.*, this issue],

$$R_{360} = 0.394 - 0.217\mu_0 + (0.684 + 0.173\mu_0)R_{\text{VIS}}, \quad (8)$$

where μ_0 is the cosine of solar zenith angle.

Ozone band-mean transmittance is calculated by exponential sum fitting:

$$T_{O_3, \text{eff}} = \sum_{i=1}^5 W_i \exp(-k_i u / \mu_0), \quad (9)$$

where u is total ozone amount in atm cm. The coefficients W_i

and k_i were tabulated separately for total UV-B and erythemal UV at each spectral band (i) [Li *et al.*, this issue].

4. Comparison Between Satellite Estimation and Ground Observation

The retrieving algorithm requires extraterrestrial incoming solar irradiance, total ozone amount, TOA albedo, aerosol optical depth and single-scattering albedo, and surface albedo. The extraterrestrial solar irradiance was taken from the solar spectrum recommended by WMO [Fröhlich and London, 1986]. Total ozone amount is available from the TOMS level-2 data set. Surface UV-B albedo is assumed to be 0.04 for Toronto and 0.03 for other stations, according to the monthly mean surface UV reflectivity product derived from Nimbus TOMS data [Herman and Celarier, 1997; Eck *et al.*, 1987] and some land surface observations reported by Blumthaler and Ambach, [1988] and Feister and Grewe [1995]. TOA albedos were computed from both Meteor-3 TOMS radiance measurement at 360 nm and NOAA AVHRR visible channel data.

Aerosol optical depth data were derived from routine measurements of direct UV irradiance (normal direct Sun total ozone measurements) made about every 20 min during the day between 1992 and 1994 for Toronto. To derive aerosol optical depth from these measurements requires the use of Langley extrapolation plot of zero air mass to determine the response of the instrument outside the atmosphere. Langley plots were carried out at Mauna Loa Observatory in 1991 and 1997 at the five operational wavelength settings of the Brewer instrument [Kerr *et al.*, 1995] and are similar to those described by Bais [1997]. The inferred optical depth is only valid for clear-sky conditions. Cloudy data were screened out by examining the temporal variability based on standard deviations computed from 10 consecutive measurements. Figure 1 shows the temporal variation and frequency distribution of aerosol optical depths in Toronto. Instantaneous values were used only when aerosol optical measurements were available. For others, the mean value of 0.31 was substituted. Somewhat ad hoc assumptions were made for aerosol optical depths at other stations due to the lack of measurements. For Winnipeg and Edmonton it was set to be 0.2, and 0.1 for the remaining remote stations. A continental aerosol model with single-scattering albedo 0.95 was applied to all stations. Uncertainties in the estimated UV fluxes due to aerosol and other input variables are discussed later.

It should be borne in mind that ground-based UV measurements also suffer from uncertainties. The most notable and widely recognized source of uncertainty for the Brewer instruments lies in the cosine correction. As the angular response of the instrument to incident solar radiance does not follow the ideal cosine function, there is a small but systematic difference between measured and true values. A correction for the effect was determined following the method of Bais *et al.* [1998] that corrected the measurements from a Brewer instrument deployed in Greece. A mean correction factor of 6% was derived, similar to those reported by Krotkov *et al.* [1998] and obtained by J. R. Herman (private communication, 1998). Therefore an increase of 6% was made to the Brewer data. This is just a nominal correction that is intended to remove the systematic error in the data to the first order of approximation. The actual correction value would be subject to change depending on the sky illumination condition.

For the sake of comparison, satellite and surface data were

matched in both time and space. The match criteria are (1) a ground station is within the footprint of a satellite pixel and is located within 30 km of the center of the pixel for cloudy conditions and 50 km for cloud-free skies; (2) time difference between satellite and ground observation is less than 7 min, which is half of the interval between the measurements made by the Toronto Brewer 14. If more than one ground measurement satisfies these criteria, the measurement with SZA closest to that of corresponding satellite pixel is retained. The comparison is limited to snow-free data obtained primarily between May and September to avoid large uncertainty in the specification of surface albedo. Note that the algorithm itself is valid for any surface, provided that surface albedo is known [Li *et al.*, this issue].

The comparisons for surface total UV-B and EUV dose rate between satellite estimation and ground observation are shown in Figures 2a and 2b, respectively, for all stations under all-sky conditions from 1992 to 1994. The mean and standard differences (or standard deviation) are 0.033 and 0.287 W/m², respectively, for surface total UV-B and 3.04 and 12.0 mW/m², respectively, for EUV. The large standard differences may result from the match between satellite and surface observations. Note that a satellite observation represents a value av-

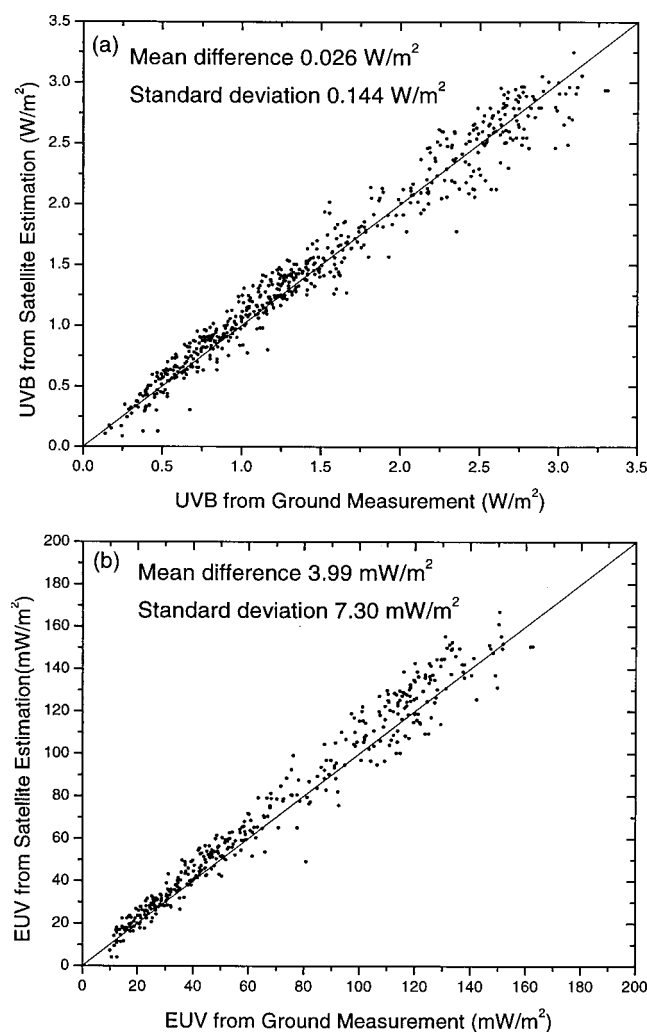


Figure 3. Same as Figure 2 except for clear-sky conditions only.

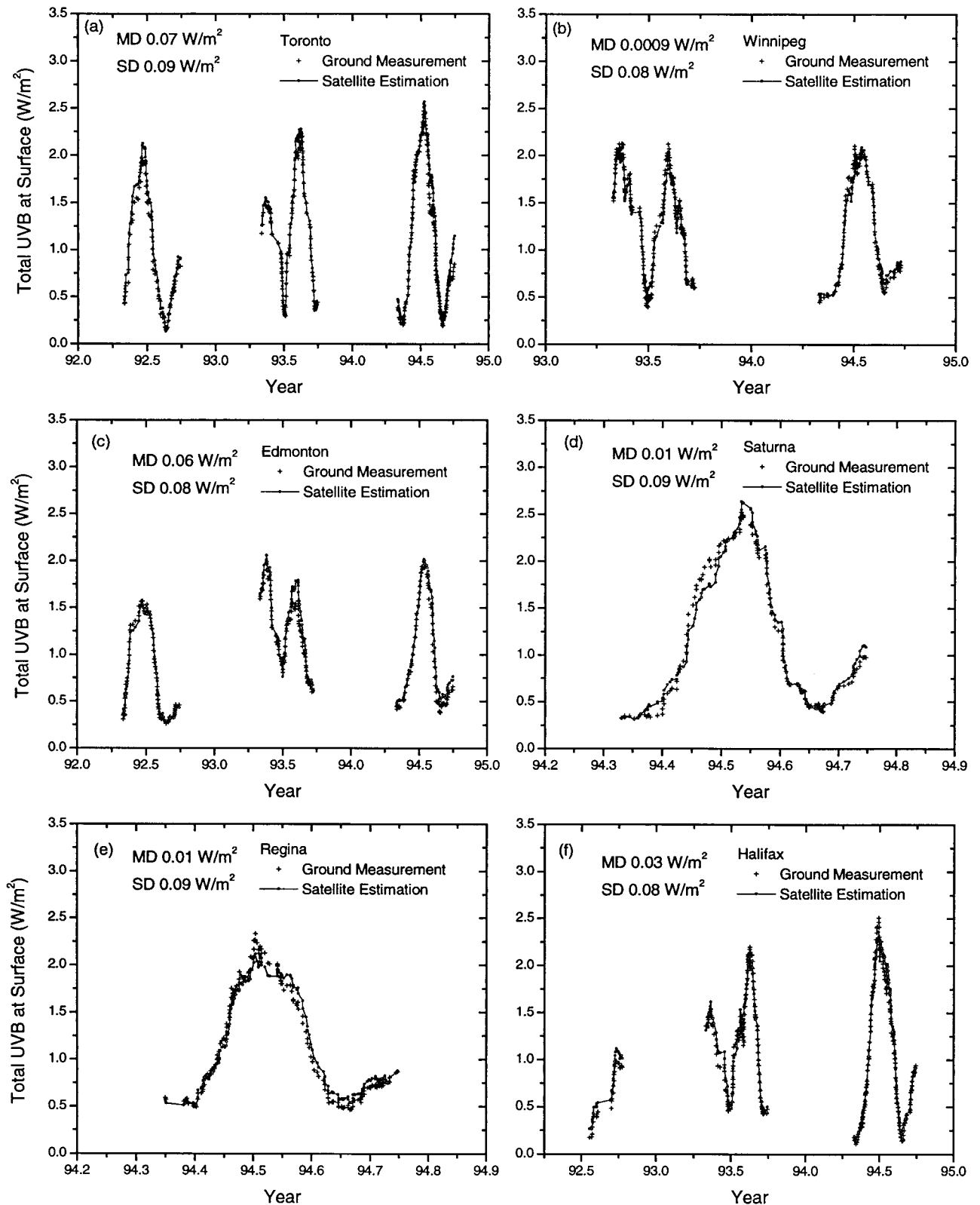


Figure 4. Comparisons of 10-day running mean surface total UV-B between satellite estimation and ground measurement at all Canadian UV stations. Mean and standard differences (MD and s.d.) are also given.

eraged over an area of $50 \times 50 \text{ km}^2$ or larger, while a ground measurement usually corresponds to a much smaller area. For a nonhomogeneous cloudy scene, the point-based ground observations may be higher or lower than the aerial mean satel-

lite-based estimates, especially for broken clouds such as cumulus. For example, *Mims and Frederick* [1994] observed a cloudy sky UV measurement that is about 20% higher than the clear-sky counterpart in the presence of a cumulus cloud dur-

ing the 1994 Hawaii Ultraviolet Survey. This could occur when the sunlight was not obscured and the sunlight scattering from cloud sides enhances UV flux reaching the surface. Of course, the opposite may be the case when the Sun is obscured by a small cloud in an otherwise clear sky.

The mismatch between satellite and surface observations should pose a much less serious problem for a clear-sky comparison. To test this, we identified homogenous clear scenes in a series of steps. TOMS UV reflectivity data were first used to separate cloudy and clear data as a first approximation. According to *Eck et al.* [1987] and *Herman and Celarier* [1997], all measurements with reflectivity less than 0.07 are considered as being clear initially. These “clear” scenes of at least 50×50 km², however, may encompass a small fraction of cloud that could affect the ground measurements. Therefore a second test is applied using ground data of high frequency. The test was based on the ratio of ground measurement to the expected value for a clear sky in order to remove the influence of SZA. The clear-sky values are modeled for a pure molecular atmosphere. Assuming aerosol does not have a strong diurnal variation, the fluctuation of the ratio is driven mainly by cloud. Standard deviations were computed from four consecutive ground measurements. The clear-sky data identified in the first step are subject to the test that their standard deviations are less than 0.02. Third, the ratio has to be greater than 0.6 to get rid of stationary clouds. The relatively large ratio was chosen to account for potentially large loading of aerosol. The comparison for the selected clear scenes only is shown in Figure 3a for

surface total UV-B irradiance and Figure 3b for EUV. The mean difference for surface total UV-B is 0.026 W/m² and standard deviation only 0.14 W/m², which is much smaller than for all-sky conditions. Likewise, the comparisons for EUV are also improved considerably, with mean and standard differences being 3.99 and 7.3 mW m⁻², respectively. Since the validation for EUV is similar to UV-B, the following discussions are limited to the latter only.

Averaging over time or space can considerably reduce the uncertainties caused by the mismatch in time and space between satellite and surface observations, since the mismatch is basically random. Figure 4 presents the comparisons of surface UV-B following a 10-day running average of the instantaneous values at all stations under study, similar to *Eck et al.* [1995]. It is seen that satellite estimation follow very closely the fluctuations as recorded by the ground instruments at every station. The mean differences and the standard deviations are much smaller than individual values. A relatively larger discrepancies are observed for some short periods of time, e.g., the comparison for Toronto during Julian days 270 to 280 of 1994 (or 94.75 in terms of the fraction of a year) when satellite-based estimates are systematically higher than ground measurements by about 0.5 W/m². The discrepancy was later identified to be associated with unrecorded ground data errors. On the majority of the first 10 days in October 1994 for the Toronto UV station, the neutral density filter was in a wrong position, which caused considerable errors in UV measurements (*V. Fioletov*, private communication, 1998). This implies that satellite re-

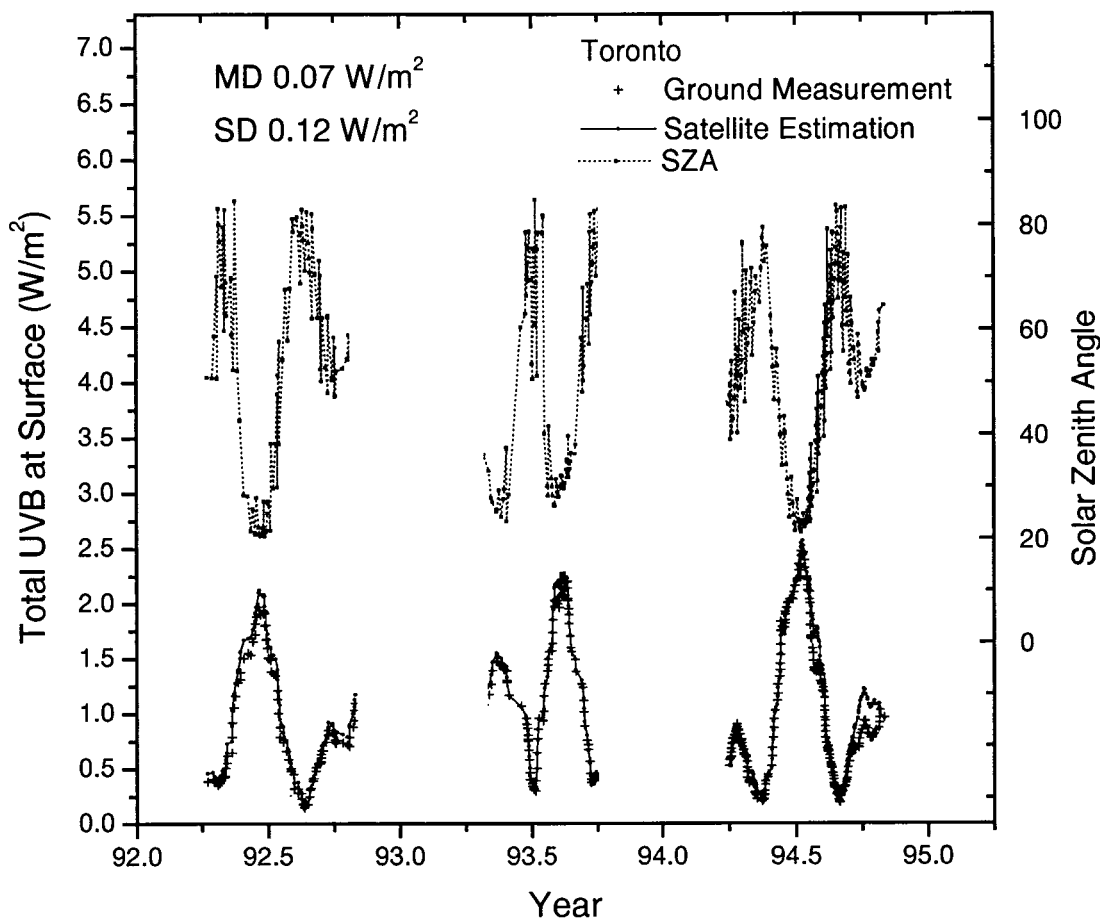


Figure 5. Comparison of variations in UV-B flux and solar zenith angle for Toronto.

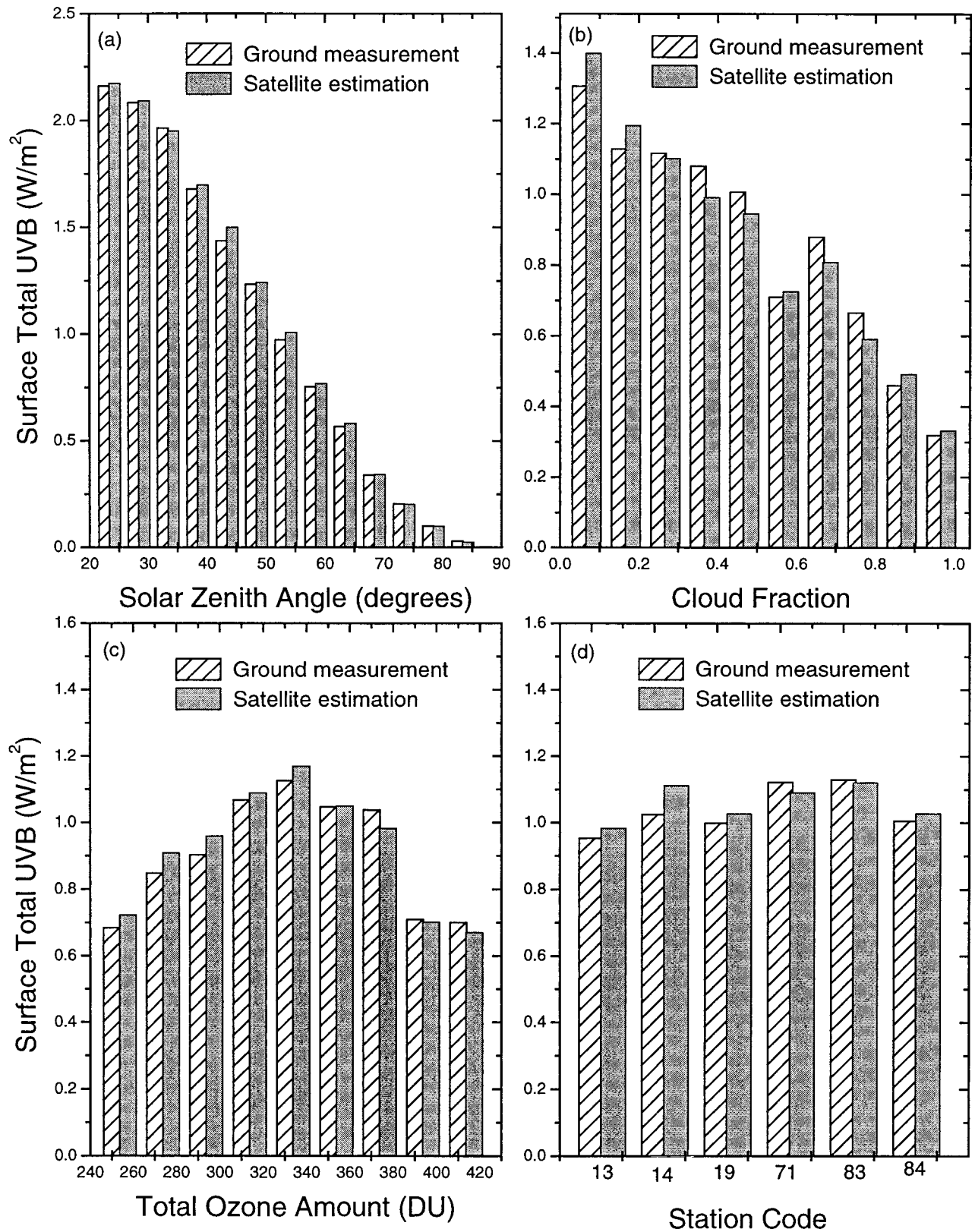


Figure 6. Comparisons of bin mean UV-B fluxes estimated from TOMS against ground measurements (1992–1994) averaged over various intervals in (a) solar zenith angle (b), cloud fraction (c), total ozone amount, and (d) stations.

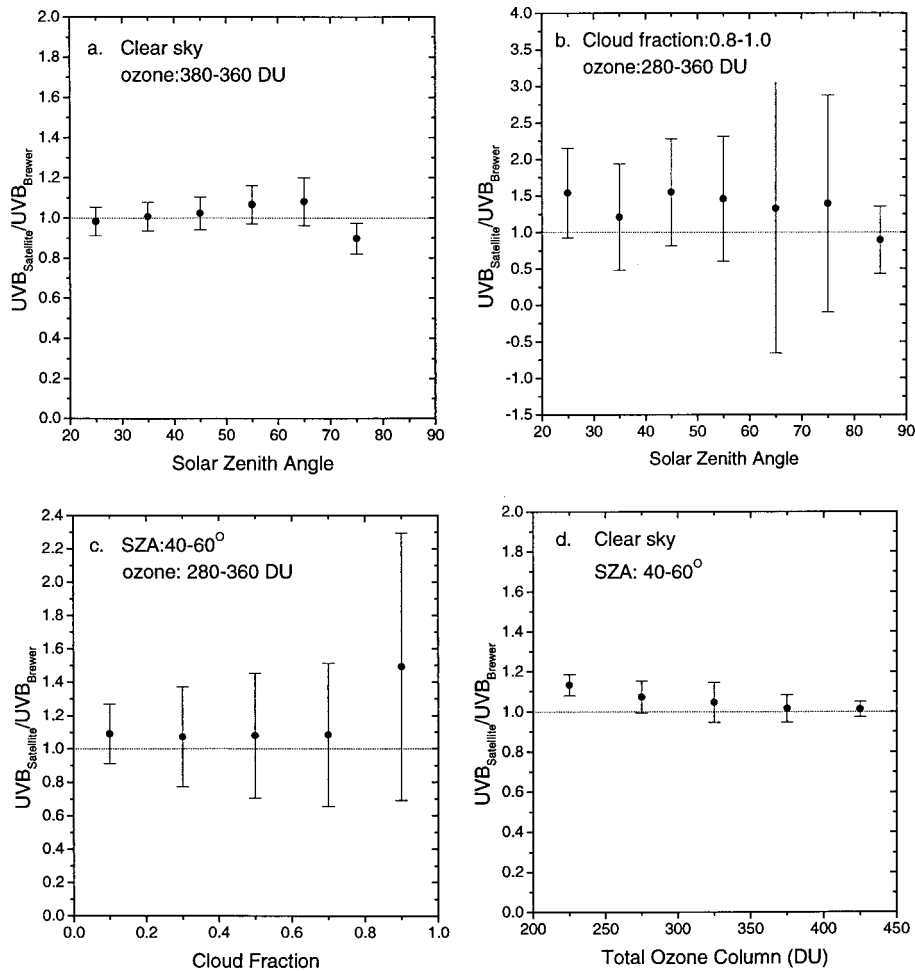


Figure 7. Ratios of estimated and observed surface UV-B fluxes averaged in the bins sorted with restrictions as specified in the plots by (a, b) solar zenith angle, (c) cloud fraction, and (d) ozone amount. Figures 7a and 7b are mostly clear and cloudy conditions, respectively.

retrieval of UV data is of such an accuracy that it could help uncover some ground measurement errors.

Note that the primary factor driving the variation as shown in Figure 4 is SZA. Figure 5 shows the comparison of variations in UV and in SZA. It is seen that the variations in surface UV-B and SZA are just opposite in phase. Although cloud usually dictates instantaneous UV-B, its effect is much reduced after averaging. To examine if various factors affecting UV-B are treated properly in the inversion algorithm, Figure 6 plots the comparisons of observed and estimated UV-B fluxes averaged over various bins sorted according to solar zenith angle, cloud fraction and total ozone amount, as well as surface stations. An apparent dependence of the comparison on any parameter may be an indicator of an inadequate treatment of that parameter in the algorithm. This seems not to be the case for all the parameters, as the agreement is ubiquitous throughout the ranges of the variables. However, the analysis may not be sufficient, given that the input variables are not necessarily independent. Such a limitation is overcome or lessened by restricting the ranges of all input values except for the one under study. Figure 7 presents the ratios of estimated and observed UV-B as functions of three input variables under restricted conditions. It follows that most of the mean ratios are less than 1.2 for clear cases. While the plots do not suggest

any significant dependence again, the large ranges of error bars due to small amount of data samples weakened the conclusion.

As discussed in section 3 and more detailed in the work of *Li et al.* [this issue], our algorithm can also employ satellite visible measurements together with ozone data. This is tested with NOAA AVHRR data acquired in Canada in 1994, in combination with TOMS level-3 ozone product. The AVHRR data were used to derive TOA UV albedos at 360 nm following spectral and angular corrections as mentioned earlier. Cloud classification required to apply the ERBE ADMs is based on the criteria of *Gutman et al.* [1987, 1991]. Other procedures for the comparison are the same as for using TOMS data. The results of the comparison are presented in Figure 8. Overall, they look similar to those for using TOMS data. The mean difference for total UV-B is 0.012 W/m^2 , and standard difference is 0.24 W/m^2 , while those for EUV are 4.1 and 9.9 mW/m^2 , respectively. The slightly lower standard deviations are presumably due to the smaller pixel size of AVHRR pixels which allows for a better match in space. On the other hand, the differences are not significant, as the cloud scale is usually much larger than 1 km.

The above comparison results should be comprehended in light of numerous uncertainties in both the input data and the surface measurements. Although the relative variation in ex-

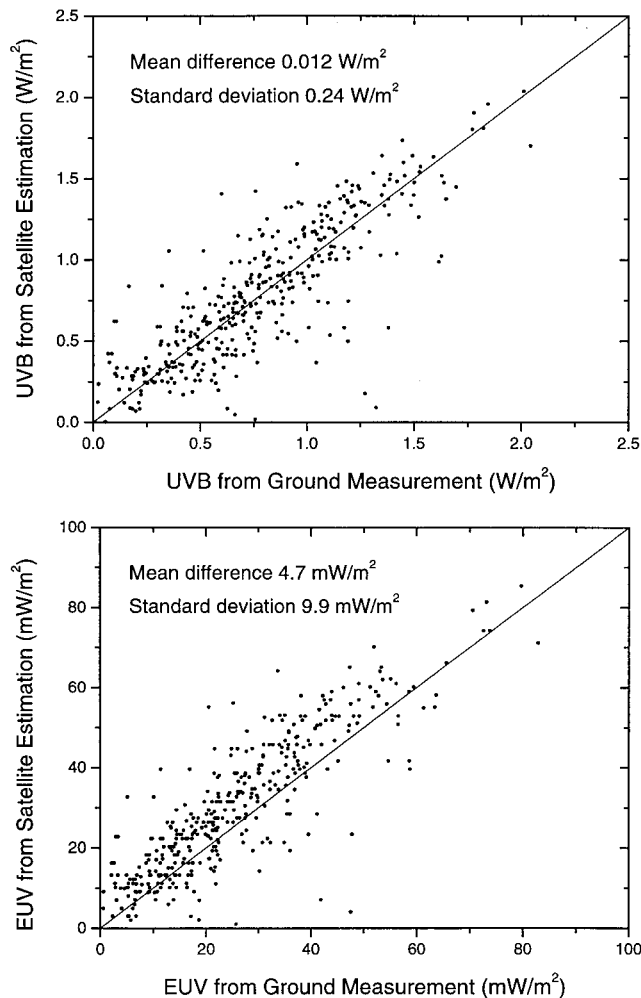


Figure 8. Same as Figure 2 but using AVHRR satellite data.

terrestrial UV-B solar irradiance is as little as 1% over the solar cycle [Rottman and Woods, 1997], the absolute accuracy is uncertain to within 3%, as suggested by the discrepancy between various observations such as the Solar Stellar Irradiance Comparison Experiment (SOLSTICE), the Solar Ultraviolet Spectral Irradiance Monitor (SUSIM), and the solar backscattered ultraviolet/model 2 (SBUV/2) [Cebula *et al.*, 1996; Woods *et al.*, 1996; Rottman *et al.*, 1993; Brueckner *et al.*, 1993; Deland and Cebula, 1998]. The surface albedos chosen according to the studies of Eck *et al.* [1987], Herman *et al.*, [1997], and Blumthaler and Ambach, [1988] are subject to an uncertainty of 2%. The input of ozone amount from TOMS may lead to more random uncertainty than to the mean difference, as a comparison between TOMS-derived and Brewer-measured total ozone amount showed a very small difference in the mean value but a much larger standard deviation. This is likely to be the case for aerosol, but we have much less confidence in correcting this factor due to the lack of knowledge on aerosol absorption. As elucidated by Li *et al.* [this issue], the performance of the algorithm is not affected by aerosol scattering but impaired strongly by aerosol absorption. Aerosols from forest fires can be very absorptive and thus alter the retrieval significantly. Forest fire in Canadian boreal forest is quite serious in the summer of 1994 [Li *et al.*, 1997]. Li and Kou [1998] investigated the effect of fire smoke on visible solar radiation mea-

sured in a remote boreal forest site in western Canada throughout the summer of 1994. They found that smoke reduced visible solar radiation at the surface by 6% on average and up to 20–25% for some cases. Smoke may have a similar influence on surface UV-B.

As for the ground measurements, the accuracy of instrument absolute calibration and cosine response are two major sources of uncertainty that matter most to the mean difference. The calibration for the Brewer instruments is accurate to within 6–7% [Wardle and Kerr, 1996]. The systematic error induced by the angular response that deviates from the cosine is only roughly corrected in this study. The aforementioned uncertainties may or may not work in the same direction, and it is thus hard to give an estimate of their accumulated effect. One can be certain, however, that it is larger than the mean differences, as we found here. As a result of these numerous uncertainties, it is hard to gain further insight into the performance of the algorithm.

5. Conclusions

The algorithm of Li *et al.* [this issue] for retrieving surface total and erythemal weighted UV fluxes from satellite has been validated in this study. The major input variables of the algorithm include total ozone amounts derived from TOMS and reflected radiance measurements made by TOMS at 360 nm or by NOAA AVHRR at visible channel. The retrieved fluxes were compared against ground-based Brewer measurements at several Canadian UV stations from 1992 to 1994. The comparisons showed very small mean differences under any sky conditions and smaller standard deviations for clear skies but larger for cloudy skies. The differences show no apparent dependence on any input parameters such as solar zenith angle, TOA albedo, total ozone amount, etc. Yet the performance of the algorithm is equally good at all stations distributed across Canada.

The larger scattering of comparisons is primarily due to the uncertainty in matching data from satellite and ground-based instruments for nonhomogeneous cloudy scenes. Variations in aerosol and ozone amounts that were not resolved by the measurements are also major contributing factors to the standard differences, especially due to strong absorbing aerosols such as those from forest fires. The mean differences are affected mainly by extraterrestrial UV irradiance, surface instrument calibration and cosine correction, and surface albedo. The magnitudes of the uncertainties in these variables are larger than the mean differences found here. As the development of the inversion algorithm was based entirely on the physics of UV radiative transfer and none are derived from observation data, its performance as revealed here is quite encouraging.

Acknowledgments. We are grateful to Pu Bu Ci Ren and G. Fedosejevs at the Canada Centre for Remote Sensing (CCRS) for technical and editorial assistance; V. Fioletov and B. McArthur at the Atmospheric Environment Service (AES) offered some valuable comments.

References

- Bais, A. F., Absolute spectral measurements of direct solar ultraviolet irradiance with a Brewer spectrophotometer, *Appl. Opt.*, 36, 5199–5204, 1997.
- Bais, A. F., S. Kazadzis, D. Balis, C. S. Zerefos, and Mario Blumthaler,

- Correcting global solar ultraviolet spectra recorded by a Brewer spectroradiometer for its angular response error, *Appl. Opt.*, *37*, 6339–6344, 1998.
- Bigelow, D. S., J. R. Slusser, A. F. Beaubien, and J. H. Gibson, The USDA ultraviolet radiation monitoring program, *Bull. Am. Meteorol. Soc.*, *79*, 601–615, 1988.
- Blumthaler, M., and W. Ambach, Solar UVB-albedo of various surfaces, *Photochem. Photobiol.*, *48*, 85–88, 1988.
- Bojkov, R., L. Bishop, W. J. Hill, G. C. Reinsel, and G. C. Tiao, A statistical trend analysis of revised Dobson total ozone data over the northern hemisphere, *J. Geophys. Res.*, *95*, 9785–9807, 1990.
- Booth, G. E., T. B. Lucas, T. Mestechkina, J. R. Tusson IV, D. A. Neuschuler, and J. H. Morrow, *NSF Polar Programs UV Spectroradiometer Network 1993–1994 Operating Report*, 223 pp., Antarc. Support Assoc. and the Natl. Sci. Found. by Bios. Instrum., San Diego, Calif. 1995.
- Brueckner, G. E., K. L. Edlow, L. E. Floyd IV, J. L. Lean, and M. E. Van Hoosier, The Solar Ultraviolet Spectral Irradiance Monitor (SUSIM) on board the Upper Atmospheric Research Satellite (UARS), *J. Geophys. Res.*, *98*, 10,695–10,711, 1993.
- Caldwell, M. M., L. B. Camp, C. W. Warner, and S. D. Flint, Action spectra and their key role in assessing biological consequences of solar UV-B radiation change, *Stratospheric Ozone Reduction, in Solar Ultraviolet Radiation and Plant Life*, edited by R. C. Worrest and M. M. Cadwell, pp. 87–111, Springer-Verlag, New York, 1986.
- Cebula, R. P., G. O. Thuillier, M. E. Van Hoosier, E. Hilsenrath, M. Herse, G. E. Brueckner, and P. C. Simon, Observation of the solar irradiance in the 200–350 nm interval during the ATLAS-1 mission: A comparison among three sets of measurements-SSBUV, SOLSPEC, and SUSIM, *Geophys. Res. Lett.*, *23*, 289–292, 1996.
- Cihlar, J., and P. M. Teillet, Forward piecewise linear model for quasi-real time processing of AVHRR data, *Can. J. Remote Sens.*, *21*, 22–27, 1995.
- Dave, J. V., Meaning of successive iteration of the auxiliary equation of radiative transfer, *Astrophys. J.*, *140*, 1292–1303, 1964.
- Deland, M. T., and R. P. Cebula, NOAA 11 solar backscatter ultraviolet, model 2 (SBUV/2) instrument solar spectral irradiance measurements in 1989–1994, 2, Results, validation, and comparisons, *J. Geophys. Res.*, *103*, 16,251–16,273, 1998.
- Eck, T. F., P. K. Bhartia, P. H. Wang, and L. L. Stowe, Reflectivity of Earth's surface and clouds in ultraviolet from satellite observations, *J. Geophys. Res.*, *92*, 4287–4296, 1987.
- Eck, T. F., P. K. Bhartia, and J. B. Kerr, Satellite estimation of spectral UVB irradiance using TOMS derived total ozone and UV reflectivity, *Geophys. Res. Lett.*, *22*, 611–614, 1995.
- Farman, J. C., B. G. Gardiner, and J. D. Shanklin, Large losses of total ozone in Antarctica reveal seasonal ClO_x No_x interaction, *Nature*, *315*, 207–210, 1985.
- Feister, U., and R. Grewe, Spectral albedo measurements in the UV and visible region over different types of surfaces, *Photochem. Photobiol.*, *62*, 736–744, 1995.
- Fröhlich C., and J. London, Revised instruction manual on radiation instruments and measurements, *WMO Tech. Note 149*, World Meteorol. Organ., Geneva, 1986.
- Gutman, G., Vegetation indices from AVHRR: An update and future prospects, *Remote Sens. Environ.*, *35*, 121–136, 1991.
- Gutman, G., D. Tarpley, and G. Ohring, Cloud screening for determination of land surface characteristics in a reduced resolution satellite data set, *Int. J. Remote Sens.*, *8*, 859–870, 1987.
- Herman, J. R., and E. A. Celarier, Earth surface reflectivity climatology at 340–380 nm from TOMS data, *J. Geophys. Res.*, *102*, 28,003–28,011, 1997.
- Herman, J. R., et al., Meteor-3 Total Ozone Mapping Spectrometer (TOMS) Data Products User's Guide, *NASA Ref. Publ.*, Washington, D. C., 1996.
- Kerr, J. B., and C. T. McElroy, Evidence for large upward trends of ultraviolet-B radiation linked to ozone depletion, *Science*, *262*, 1032–1034, 1993.
- Kerr, J. B., C. T. McElroy, D. I. Wardle, R. A. Olafson, and W. F. J. Evans, The automated Brewer spectrophotometer, Proceedings of the Quadrennial Symposium on Atmospheric Ozone, edited by C. S. Zerefos and A. Ghazi, pp. 396–401, D. Reidel, Norwell, Mass., 1995.
- Krotkov, N. A., P. K. Bhartia, J. R. Herman, V. Fioletov, and J. Kerr, Satellite estimation of spectral surface UV irradiance in the presence of tropospheric aerosols, 1, Cloud-free case, *J. Geophys. Res.*, *103*, 8779–8793, 1998.
- Li, Z., On the angular correction of satellite radiation measurement: The performance of ERBE angular dependence model in the Arctic, *Theor. Appl. Climatol.*, *54*, 235–248, 1996.
- Li, Z., and L. Kou, The direct radiative effect of smoke aerosols on atmospheric absorption of visible sunlight, *Tellus, Ser. B*, *50*, 543–554, 1998.
- Li, Z., J. Cihlar, L. Moreau, F. Huang, and B. Lee, Monitoring fire activities in the boreal ecosystem, *J. Geophys. Res.*, *102*, 29,611–29,624, 1997.
- Li, Z., P. Wang, and J. Cihlar, A simple and efficient method for retrieving surface UV radiation dose rate from satellite, *J. Geophys. Res.*, this issue.
- Lubin, D., and E. H. Jensen, Effects of clouds and stratospheric ozone depletion on ultraviolet radiation trends, *Nature*, *377*, 710–713, 1995.
- Madronich, S., and F. R. deGrujil, Skin cancer and UV radiation, *Nature*, *366*, 23, 1993.
- Mayer, B., and G. Seckmeyer, All-weather comparison between spectral and broadband (Robertson-Berger) UV measurement, *Photochem. Photobiol.*, *64*, 792–799, 1996.
- Mayer, B., G. Seckmeyer, and A. Kylling, Systematic long-term comparison of spectral UV measurement and UVSPEC modeling results, *J. Geophys. Res.*, *102*, 8755–8767, 1997.
- McKenzie, R. L., M. Blumthaler, R. Booth, S. B. Diaz, J. E. Frederick, T. Ito, S. Madronich, and G. Seckmeyer, Surface ultraviolet radiation, in *UNEP/WMO Scientific Assessment of Ozone Depletion: 1994, WMO Rep. 37*, edited by D. L. Albritton, R. T. Watson, and P. J. Aucamp, pp. 9.1–9.22, WMO Global Ozone Res. and Monit. Proj., Geneva, 1995.
- McKinlay, A. F., and B. L. Diffey, A reference action spectrum for ultraviolet induced erythema in human skin, in *Human Exposure to Ultraviolet Radiation: Risks and Regulations*, edited by W. R. Passchier and B. F. M. Bosnjakovic, pp. 83–87, Elsevier, New York, 1987.
- McPeters, R. D., et al., Nimbus-7 Total Ozone Mapping Spectrometer (TOMS) Data Products User's Guide, *NASA Ref. Publ.*, Washington, D. C., 1993.
- McPeters, R. D., S. M. Hollandsworth, L. E. Flynn, J. R. Herman, and C. J. Seftor, Long-term ozone trends derived from the 16-year combined Nimbus 7/Meteor 3 TOMS Version 7 record, *Geophys. Res. Lett.*, *23*, 3699–3702, 1996.
- Mims, F. M., and J. E. Frederick, Cumulus clouds and UV-B, *Nature*, *371*, 291–291, 1994.
- Rottman, G. J., and T. N. Woods, SOLSTICE measurement of solar ultraviolet irradiance, 120 to 420 nm, IRS'96, in *Current Problems in Atmospheric Radiation*, edited by W. L. Smith and K. Stamnes, A. Deepak, Hampton, Va., 1997.
- Rottman, G. L., T. N. Woods, and T. P. Sparn, Solar Stellar Irradiance Comparison Experiment, 1, Instrument design and operation, *J. Geophys. Res.*, *98*, 10,667–10,678, 1993.
- Setlow, R. B., The wavelength in sunlight effective in producing skin cancer: A theoretical analysis, *Proc. Natl. Acad. Sci., U. S. A.*, *71*, 3363–3366, 1974.
- Solomon, S., The mystery of the Antarctic ozone "hole", *Rev. Geophys.*, *26*, 131–148, 1988.
- Suttles, J. T., R. N. Green, P. Minnis, G. L. Smith, W. F. Staylor, B. A. Wielicki, I. J. Walker, D. F. Ypung, V. R. Taylor, and L. L. Stowe, Angular radiation models for Earth-atmosphere system, in *Short-wave Radiation*, vol. 1, *NASA Ref. Publ.*, 1184, 114 pp., 1988.
- Wang, P., Modelling and measurement of solar ultraviolet radiation, Ph.D. thesis, L'Univ. des Sci. et Technol. de Lille, Lille, France, 1995.
- Wang, P., and J. Lenoble, Comparison between measurements and modeling of UV-B irradiance for clear sky: A case study, *Appl. Opt.*, *33*, 3964–3971, 1994.
- Wang, P., and J. Lenoble, Influence of clouds on UV irradiance at ground level and backscattered exitance, *Adv. Atmos. Sci.*, *13*, 217–228, 1996.
- Wardle, D. I., and J. B. Kerr, WUDC documents, World Ozone and Ultraviolet Radiat. Data Cent., 1996.
- Wardle, D. I., E. W. Hare, D. V. Barton, and C. T. McElroy, The world ozone and ultraviolet radiation data centre, in paper presented at the Quadrennial Ozone Symposium, l'Aquila, Italy, September 1996.

- Wardle, D. I., J. B. Kerr, C. T. McElroy, and D. R. Francis, *Ozone Science: A Canadian Perspective on the Changing Ozone Layer*, 119 pp., Environ. Can., Dartmouth, N. S., 1997.
- Webb, A., Advances in solar ultraviolet spectroradiometry, *Air Pollut. Res. Rep.*, 63, Eur. Comm., 1997.
- Woods, T. N., et al., Validation of the UARS solar ultraviolet irradiances: Comparison with the ATLAS 1 and 2 measurements, *J. Geophys. Res.*, 101, 9541–9569, 1996.
- World Meteorological Organization (WMO), *Scientific Assessment of Stratospheric Ozone: 1989*, WMO Rep. 30, Global Ozone Res. and Monit. Proj., Geneva, 1994.

J. Cihlar, Z. Li, and P. Wang, Canada Centre for Remote Sensing, 588 Booth Street, Ottawa, Canada, K1A 0Y7. (li@ccrs.nrcan.gc.ca)
J. Kerr and D. I. Wardle, Atmospheric Environment Service, 4905 Dufferin Street, Downsview, ON, M3H 5T4 Canada.

(Received February 25, 1999; revised June 2, 1999;
accepted June 4, 1999.)